

Multi-lane Detection Using Instance Segmentation and Attentive Voting

Donghoon Chang¹, Vinjohn Chirakkal², Shubham Goswami^{1,*}, Munawar Hasan¹, Taekwon Jung²,
Jinkeon Kang^{1,3}, Seok-Cheol Kee⁴, Dongkyu Lee⁵, Ajit Pratap Singh¹

¹Department of Computer Science, IIIT-Delhi, India

²Springcloud Inc., Korea

³Center for Information Security Technologies (CIST), Korea University, Korea

⁴Smart Car Research Center, Chungbuk National University, Korea

⁵Department of Smart Car Engineering, Chungbuk National University, Korea

* Corresponding author

Abstract: Autonomous driving is becoming one of the leading industrial research areas. Therefore many automobile companies are coming up with semi to fully autonomous driving solutions. Among these solutions, lane detection is one of the vital driver-assist features that play a crucial role in the decision-making process of the autonomous vehicle. A variety of solutions have been proposed to detect lanes on the road, which ranges from using hand-crafted features to the state-of-the-art end-to-end trainable deep learning architectures. Most of these architectures are trained in a traffic constrained environment. In this paper, we propose a novel solution to multi-lane detection, which outperforms state of the art methods in terms of both accuracy and speed. To achieve this, we also offer a dataset with a more intuitive labeling scheme as compared to other benchmark datasets. Using our approach, we are able to obtain a lane segmentation accuracy of 99.87% running at 54.53 fps (average).

Keywords: Autonomous Driving, Lane Detection, Segmentation, Deep Learning, Computer Vision.

1. INTRODUCTION

In recent years, self-driving cars have started becoming a reality due to the advances in deep learning and hardware capabilities of various sensors and control modules. It is seeking the attention of both industry and academic research as it covers a wide range of research areas from computer vision to signal processing and many more. Multi-lane detection is one of the vital driver-assist features in these autonomous vehicles, which plays a crucial role in path planning and the decision-making process of autonomous vehicles. It introduces several challenges and requires to be highly accurate and to work in real-time.

1.1 Related Work

A variety of lane detection methods have been proposed starting from the traditional methods using hand-crafted features ([1], [2], [3], [4], [5], [6]) to the modern state of the art end-to-end trainable deep architectures ([7], [8], [9], [10], [11], [12]). Spatial CNN [11] and end-to-end lane segmentation [12] use CNN-based approach to exploit the spatial information in a road scene and try to develop an understanding of a road scene. The key issue with these architectures is that they are not trained in adverse conditions, and the dataset used for training comes from traffic constrained environment and also has a non-intuitive annotation procedure as it is discussed further in Section 2.

1.2 Motivation

Semantic segmentation of a road scene involves a variety of objects with different sizes. The encoders in segmentation network architectures like [13], [14], and [15] are deep enough that neurons in its last layer have a re-

ceptive field greater than or equal to the size of the input images. In lane segmentation, lane markings are placed on a road; hence, there is an upper bound on the size of lane markings. It can be exploited by limiting the depth of the encoder, by increasing the inference speed and by decreasing learnable parameters in lane segmentation network. Apart from lane segmentation, the state-of-the-art method like [12] strongly depends on the road scene environment to generate the embeddings for clustering. Intuitively, using lane markings alone for multi-lane detection makes more sense. This also reduces the need to adequately capture the background diversity and dependencies, such as traffic and geometric constraints. For example, VPGNet [16] predicts vanishing point on the input frame for guiding lane and road marking detection and recognition in adverse circumstances this introduces more training data to capture the input diversity for vanishing point prediction and also vanishing point works well on straight roads but not on curving roads or roundabouts.

2. DATASET

There are various available road scene datasets with pixel-level annotations; CamVid (Cambridge-driving Labeled Video Database, [17]), Cityscapes [18], KITTI dataset [19], Caltech lane dataset [20] and tuSimple [21]. Apart from tuSimple, others contain a small set of images with lane marking annotations. On the other hand, datasets like tuSimple are very traffic-constrained (light traffic and clear lane markings in [11]) and its annotations are comprised of continuous lane curves starting from the bottom of the input frame till the horizon and even passing over the vehicles as shown in Fig. 1 (Top). The issue with such labeling approach is that only lane marking

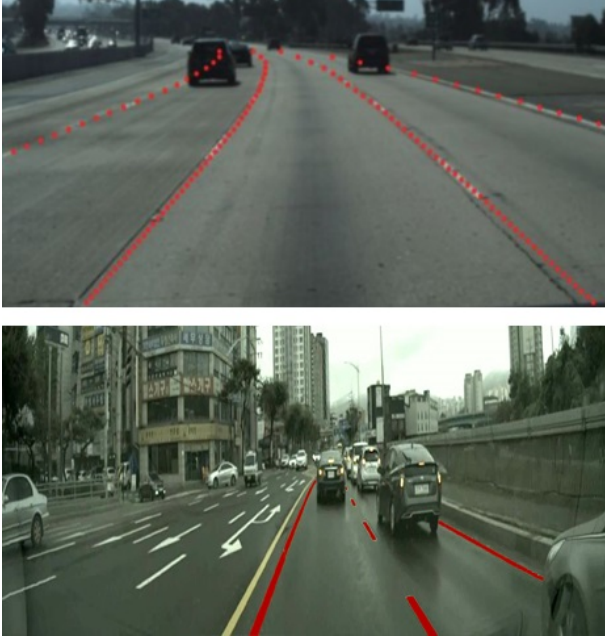


Fig. 1: Top: an annotated sample frame from tuSimple dataset. Bottom: an annotated sample frame from our dataset.

pixels should be marked as lane markings, and one shall not assume them anywhere else; otherwise, this can cause issues by predicting false positives in high traffic scenarios [11].

We collected a small dataset which includes city traffic on cloudy days capturing conditions ranging from water reflection on the road to moving wipers on the windshield. From this collected dataset, we annotated 5,000 frames in a pixel-wise manner without carrying any assumptions, i.e., only visible lane markings aligned in the direction of the movement of the vehicle, as shown in Fig. 1 (Bottom).

3. METHODOLOGY

The preprocessing of input frames involves cropping majority of the sky portion and car dashboard. Afterward, the frame is resized to the resolution of 360x480. This frame is then fed to the lane marking segmentation network, which segments out the visible lane marking pixels followed by detecting instances of segmented lane markings using graph-based methods. Perspective transformation (bird’s eye view) is then applied to the instance segmented output followed by attentive voting based clustering method and polynomial curve fitting, which provides the final output. The architecture diagram is given in Fig.2.

3.1 Lane segmentation

We follow CNN-based approach [22] to create lane segmentation network with *strided convolutions* and *strided de-convolutions* with *relu* [23] activation in hidden units and we propose the customized soft dice loss

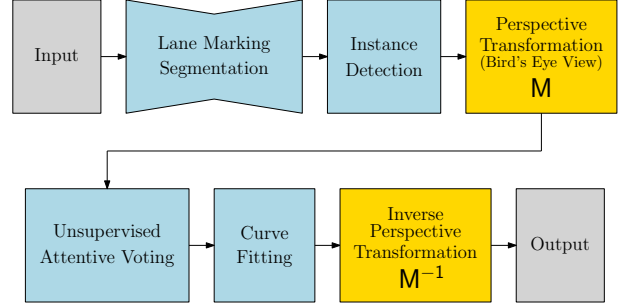


Fig. 2: Architecture Diagram

[24] to penalize false positives by modifying the ground truth (Eq. (1)) in the numerator of $Loss_{custom}$ (Eq. (3)). The strided convolution is used to increase the receptive field.

Fig. 3 shows the accuracy, loss plot and softmax loss used as the evaluation metrics. Table 1 shows the lane segmentation network architecture. We have exploited the upper bound on the size of lane marking and the last layer of encoder captures a receptive field of $63 \times 63 \text{ pixel}^2$ on the original input.

$$\hat{y}_{gt}[i][j][k] = -\alpha \text{ where } y_{gt}[i][j][k] = 0 \quad (1)$$

$$mean(A) = \frac{\sum_i \sum_j A_{i,j}}{\|A\|} \quad (2)$$

$$Loss_{custom}(y_{gt}, y_{pred}) = - \sum_{k=1}^c \frac{2 * mean(\hat{y}_{gt}^k \circ y_{pred}^k) + \epsilon}{mean(y_{gt}^k \circ y_{gt}^k) + mean(y_{pred}^k \circ y_{pred}^k) + \epsilon} \quad (3)$$

In Eq. (1), i and j represent the spatial index. k represents the channel index of the output, where $k = 1$ and $k = 2$ are the channel for background (non-lane marking) and lane marking, respectively. In Eq. (3), c is the total number of channels in the ground truth/prediction, y_{pred}^k , y_{gt}^k and \hat{y}_{gt}^k are the k -th channel values of predicted output, the ground truth and modified ground truth (Eq. (1)), respectively. We achieved the best results with $\alpha = 10^{-2}$ and $\epsilon = 10^{-5}$ after tuning them respectively while training.

3.2 Instance detection and bird’s eye view

We use the customized Breadth-first search to detect all the distinct instances of lane markings in the output of the lane segmentation network. Perspective transformation is then applied to provide ease of voting in clustering and curve fitting as the bird’s eye view reduces the degree of a polynomial. It is important because on many occasions only a few pixels are obtained for some lane markings (e.g., lane markings on road boundaries) and higher degree polynomial requires proportionally more pixels to fit; thus a lower degree polynomial helps in performing

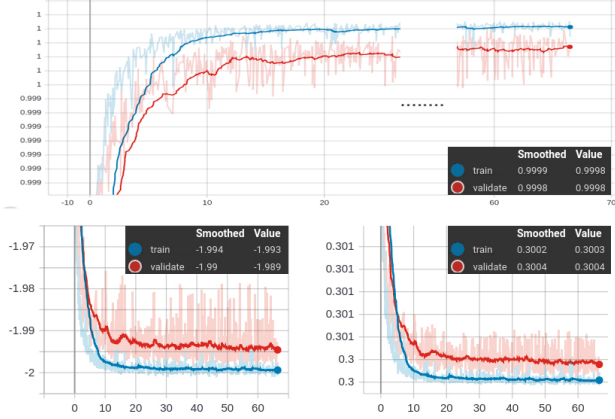


Fig. 3: Top: accuracy plot. Bottom: $Loss_{custom}$ (left) and softmax loss (right).

Table 1: Lane segmentation network architecture with fused batch normalization [25]

Layer	Input	Output
Conv2D+Relu.	360x480x3	179x239x32
Conv2D+Relu.	179x239x32	89x119x64
Conv2D+Relu.	89x119x64	44x59x128
Conv2D+Relu.	44x59x128	21x29x256
Conv2D+Relu.	21x29x256	10x14x512
Conv2DTrans.+Relu.	10x14x512	21x29x256
Conv2DTrans.+Relu.	21x29x256	44x59x128
Conv2DTrans.+Relu.	44x59x128	89x119x64
Conv2DTrans.+Relu.	89x119x64	179x239x32
Conv2DTrans.	179x239x32	360x480x2
Softmax	360x480x2	360x480x2

the better curve fitting even if the instance pixels are less in number.

3.3 Unsupervised attentive voting and curve fitting

In the bird’s eye view space, all the instances vote for their closest instance based on slope and spatial positioning of the instances. The slope and spatial positioning of an instance (i.e., lane marking) are used as spatial attention to vote for its closest lane marking, which belongs to the same lane divider. Fig. 4 shows how the attention is used to calculate the vote by giving the example of attentive voting among a pair of lane marking instances. \vec{L}_i represents the instance of lane marking. $\vec{L}_{i_{min}}$ and $\vec{L}_{i_{max}}$ are the bottom-most and the top-most pixel of lane marking L_i , respectively. The vote between two lane markings L_i and L_j as $vote(L_i, L_j)$ which is calculated by taking sum of d_1 and d_2 where d_i (for $i \in \{1, 2\}$) in Fig. 4) represents the perpendicular distance of point P with the line fitted on the pixels of lane marking L_i using normal equation (closed-form solution for linear regression [26]). If this vote is less than some threshold η , then these two instances belong to the same lane divider. This unsupervised clustering approach takes care of some mis-

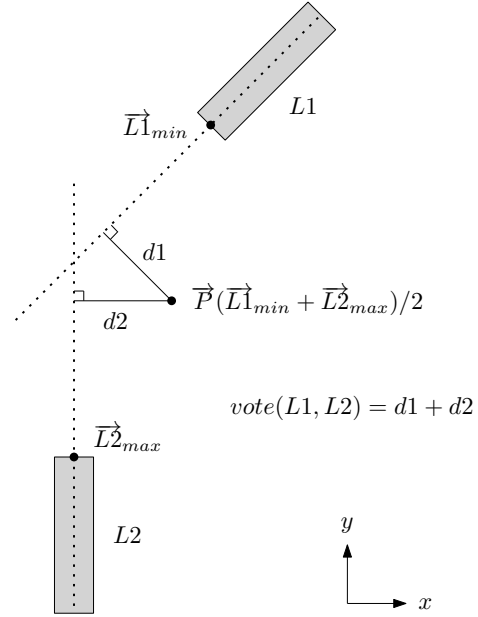


Fig. 4: The example of attentive voting between two instances of lane markings L_1 and L_2 .

classified lane marking pixels as through attentive voting the instance belonging to same lane divider are correctly grouped together, which is the expected outcome. Curve fitting for a second-degree polynomial is performed in the same bird’s eye view space on each cluster of instances and projecting this output back to original space provides the desired result.

4. EXPERIMENTS AND RESULTS

For our experiments, we ran our model on Intel Xeon(R) E5-2620 v4 processor and Nvidia RTX 2080Ti. We calculate the average inference time approximately, as shown in Table 2. It shows that the total processing time takes about 0.01833 ms. In Table 3, we calculate the accuracy of lane segmentation for the comparison. Fig. 5 shows the visual results of the proposed architecture in three different stages; the original input with ground truth (top), the output of lane segmentation network (middle), and the final output of attentive voting and curve fitting (bottom).

Table 2: Inference time (approximate average)

Task	Time (ms)	Speed (fps)
Lane segmentation	0.001449	690
Instance detection + Bird’s eye view + Attentive voting + Curve fitting	0.01688	59.21
Total	0.01833	54.535

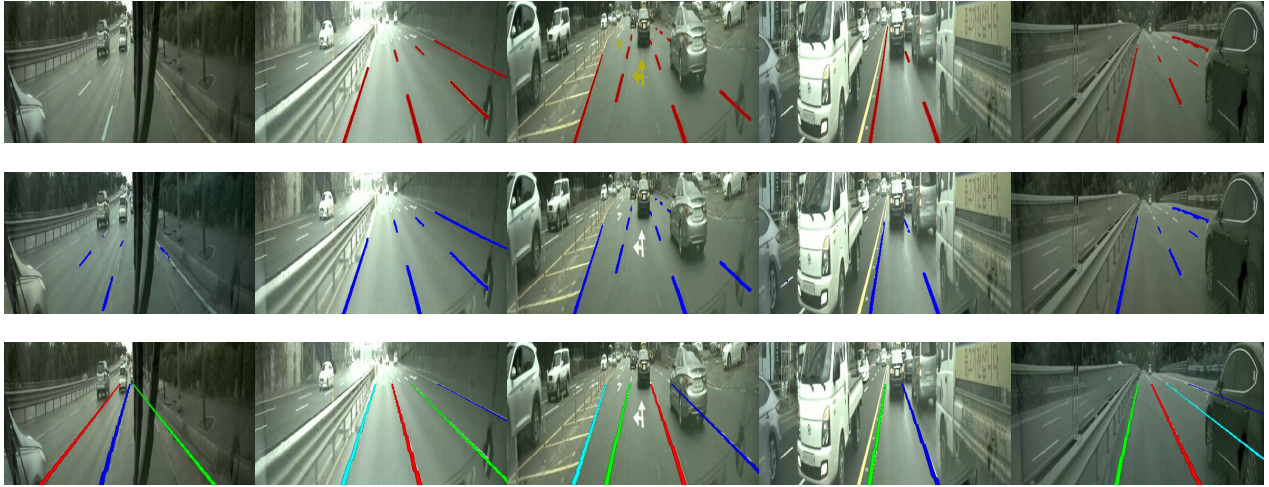


Fig. 5: Visual result. Top row: original input with ground truth. Middle row: the output of lane segmentation network. Bottom row: the final output of attentive voting and curve fitting.

Table 3: Comparison of the accuracy of lane segmentation

	Accuracy	Speed (fps)
[12]	96.4%	52.6
Ours	99.87%	54.535

5. CONCLUSION

In this paper, we proposed a novel method for multi-lane detection, which outperforms the state-of-the-art methods in terms of accuracy and speed. To this, we also offer the dataset with a more intuitive labeling scheme as compared to other benchmark datasets. Using our approach, we are able to obtain the accuracy of 99.87% at 54.53 fps.

ACKNOWLEDGEMENTS

This work was supported by Korea Institute for Advancement of Technology (KIAT) grant funded by the Korea Government (MOTIE) (N0002428, The Competency Development Program for Industry Specialist)

REFERENCES

- [1] A. Borkar, M. Hayes and M. T. Smith, "A Novel Lane Detection System With Efficient Ground Truth Generation," *IEEE Transactions on Intelligent Transportation Systems*, vol. 13, no. 1, pp. 365-374, 2012.
- [2] H. Deusch, J. Wiest, S. Reuter, M. Szczot, M. Konrad and K. Dietmayer, "A Random Finite Set Approach to Multiple Lane Detection," *IEEE Conference on Intelligent Transportation Systems*, pp. 270-275, 2012.
- [3] J. Hur, S. Kang and S. Seo, "Multi-Lane Detection in Urban Driving Environments Using Conditional Random Fields," *IEEE Intelligent Vehicles Symposium*, pp. 1297-1302, 2013.
- [4] H. Jung, J. Min and J. Kim, "An Efficient Lane Detection Algorithm For Lane Departure Detection," *IEEE Intelligent Vehicles Symposium*, pp. 976-981, 2013.
- [5] H. Tan, Y. Zhou, Y. Zhu, D. Yao and K. Li, "A novel curve lane detection based on Improved River Flow and RANSA," *IEEE Conference on Intelligent Transportation Systems*, pp. 133-138, 2014.
- [6] P.-C. Wu, C.-Y. Chang and C. H. Lin, "Lane-mark extraction for automobiles under complex conditions," *Pattern Recognition*, vol. 47, no. 8, pp. 2756-2767, 2014.
- [7] J. Kim and M. Lee, "Robust Lane Detection Based On Convolutional Neural Network and Random Sample Consensus," *Neural Information Processing*, pp. 454-461, 2014.
- [8] B. Huval, T. Wang, S. Tandon, J. Kiske, W. Song, J. Pazhayampallil, M. Andriluka, P. Rajpurkar, T. Migimatsu, R. Cheng-Yue, F. Mujica, A. Coates and A. Y. Ng, "An Empirical Evaluation of Deep Learning on Highway Driving," *CoRR*, vol. abs/1504.01716, 2015.
- [9] B. He, R. Ai, Y. Yan and X. Lang, "Accurate and robust lane detection based on Dual-View Convolutional Neural Network," *IEEE Intelligent Vehicles Symposium*, pp. 1041-1046, 2016.
- [10] J. Li, X. Mei, D. V. Prokhorov and D. Tao, "Deep Neural Network for Structural Prediction and Lane Detection in Traffic Scene," *IEEE Transactions on Neural Networks and Learning Systems*, vol. 28, no. 3, pp. 690-703, 2017.
- [11] X. Pan, J. Shi, P. Luo, X. Wang and X. Tang, "Spatial as Deep: Spatial CNN for Traffic Scene Understanding," *Thirty-Second AAAI Conference on Artificial Intelligence*, 2018.
- [12] D. Neven, B. D. Brabandere, S. Georgoulis, M. Proesmans and L. V. Gool, "Towards End-to-End

- Lane Detection: an Instance Segmentation Approach,” *IEEE Intelligent Vehicles Symposium*, pp. 286-291, 2018.
- [13] V. Badrinarayanan, A. Kendall and R. Cipolla, “SegNet: A Deep Convolutional Encoder-Decoder Architecture for Image Segmentation,” *IEEE Transactions on Pattern Analysis and Machine Intelligence*, vol. 39, no. 12, pp. 2481-2495, 2017.
- [14] T. Falk, D. Mai, R. Bensch, Ö. Çiçek, A. Abdulkadir, Y. Marrakchi, A. Böhm, J. Deubner, Z. Jckel, K. Seiwald, A. Dovzhenko, O. Tietz, C. D. Bosco, S. Walsh, D. Saltukoglu, T. L. Tay, M. Prinz, K. Palme, M. Simons, I. Diester, T. Brox and O. Ronneberger, “U-Net: deep learning for cell counting, detection, and morphometry,” *Nature Methods*, vol. 16, no. 1, 2019.
- [15] A. Paszke, A. Chaurasia, S. Kim and E. Culurciello, “ENet: A Deep Neural Network Architecture for Real-Time Semantic Segmentation,” 2016. Available: <https://arxiv.org/abs/1606.02147>
- [16] S. Lee, J. Kim, J. S. Yoon, S. Shin, O. Bailo, N. Kim, T. Lee, H. S. Hong, S. Han and I. S. Kweon, “VPGNet: Vanishing Point Guided Network for Lane and Road Marking Detection and Recognition,” *IEEE International Conference on Computer Vision*, 2017.
- [17] G. J. Brostow, J. Fauqueur and R. Cipolla, “Semantic object classes in video: A high-definition ground truth database,” *Pattern Recognition Letters*, vol. 30, no. 2, pp. 88-97, 2009.
- [18] M. Cordts, M. Omran, S. Ramos, T. Rehfeld, M. Enzweiler, R. Benenson, U. Franke, S. Roth and B. Schiele, “The Cityscapes Dataset for Semantic Urban Scene Understanding,” *IEEE Conference on Computer Vision and Pattern Recognition*, pp. 3213-3223, 2016.
- [19] A. Geiger, P. Lenz, C. Stiller and R. Urtasun, “Vision meets robotics: The KITTI dataset,” *The International Journal of Robotics Research*, vol. 32, no. 11, pp. 1231-1237, 2013.
- [20] M. Aly, “Real time Detection of Lane Markers in Urban Streets,” *IEEE Intelligent Vehicles Symposium*, p. 7-12, 2008.
- [21] TuSimple: Lane Detection Challenge. <http://benchmark.tusimple.ai>
- [22] A. Krizhevsky, I. Sutskever, G. E. Hinton, “ImageNet Classification with Deep Convolutional Neural Networks,” *Advances in Neural Information Processing Systems*, pp. 1097-1105, 2012.
- [23] V. Nair and G. E. Hinton, “Rectified Linear Units Improve Restricted Boltzmann Machines,” *Proceedings of the 27th International Conference on Machine Learning*, 2010.
- [24] C. H. Sudre, W. Li, T. Vercauteren, S. Ourselin and M. J. Cardoso, “Generalised Dice Overlap as a Deep Learning Loss Function for Highly Unbalanced Segmentations,” *Deep Learning in Medical Image Analysis and Multimodal Learning for Clinical Decision Support*, pp. 240-248, 2017.
- [25] W. Jung, D. Jung, B. Kim, S. Lee, W. Rhee and J. H. Ahn, “Restructuring Batch Normalization to Accelerate CNN Training,” 2018. Available: <https://arxiv.org/abs/1807.01702>
- [26] Bishop, Christopher M. *Pattern recognition and machine learning*. springer, 2006.